Table 8- Differences between the computed and original coordinates of check points

No. of check points	X difference (m)	Y difference (m)	Z difference (m)
1	-129.731752	-11.974557	160.179949
2	72.548069	-49.088296	-27.601637
3	-82.080482	-11.393840	328.139363
4	11.532023	11.374207	28.591644
5	101.427132	31.563932	-97.454667
6	27.624292	-34.065214	66.129042
7	124.570777	-17.617602	-143.900027
8	19.254656	-28.832136	-40.352941

Table 9- RMSE of check points obtained by DLT (method 2)

Method	X & Y RMSE of check points (m)	Z RMSE of check points (m)
DLT	124.311	10.418
	X & Y RMSE of control points (m)	Z RMSE of control points (m)
DLT	49.091	10.379

Table 10- Differences between the computed and original coordinates of check points

No. of check points	X difference (m)	Y difference (m)	Z difference (m)
1	-83.400867	-8.514500	-8.587859
2	35.946747	-84.456549	-5.897525

Table 11- The results of the proposed Radargrammetry algorithm converted to UTM projection system

Point Types	Points	X Diff. (m)	Y Diff. (m)	Height Diff. (m)	RMSE of X & Y (m)
Control Points	#1 (flat)	11.805000000051	34.933999999892	6.20172825	36.874684825686
	#2 (flat)	15.253000000026	11.571999999695	-0.3204760	19.145892326912
	#3 (flat)	57.553000000	181.9879999998	34.917059	190.87163213262
	#4 (flat)	41.386999999988	129.8030000	24.945258	136.24133946082
Check Points	#1 (flat)	104.88599999994	-98.46999999	11.182440	143.86595808576
	#2 (flat)	111.88000	-249.570999999	-64.936943	273.50103919546
	#3 (mount.)	28.233000000	-529.4859999995	-70.5161502	530.2381790144
	#4 (mount.)	-807.0990000	269.419000000	282.8959206	850.87918846461
	#5 (mount.)	-702.35700	217.20699999	327.9989647	735.1763300719
	#6 (mount.)	-34.6169999	-628.39399999	-103.013437	629.34676921774

References

Crosetto, M. & Argues Pereze F., 1999 - Radargrammetry and SAR interferometry for DEM generation: validation and data fusion. Proceedings of a Conference held 26-29 October, Toulouse, France. European Space Agency, 2000. ESA-SP vol. 450, ISBN: 9290926414, p.367.

Liu, H., Zhao Z. & Jezek, K. C., 2004 - Correction of positional errors and geometric distortions in topographic maps and DEMs using rigorous SAR simulation technique, Photogrammetric Engineering & Remote Sensing , Vol. 70, No. 9, 1031-1042

Leberl, F. W., 1990 – Radargrammetric Image Processing. Artech House.

Table 3- Point wise polynomial results

Number of nearest points	RMSE of check points using moving average	RMSE of check points using weighted distance
3	96.868	63.288
4	92.644	65.532
5	80.907	63.400
6	79.335	63.070
7	73.009	62.402
8	65.177	62.782
9	62.512	62.551
10	63.044	61.760
11	61.836	61.140
12	60.704	60.820
13	57.946	61.468
14	57.388	61.629
15	57.371	61.424

Table 4- Global polynomial results for flat area

Polynomial type	RMSE of check points (m)	RMSE of control points (m)
Linear poly.	71.556	60.673
Bilinear ploy.	67.853	36.782
Quadratic (type 1)	57.928	21.92
Quadratic (type 2)	73.486	17.598
Quadratic (type 3)	55.676	18.642
Quadratic (type 4)	58.636	15.738

Table 5- Global polynomial results for mountainous area

Polynomial type	RMSE of check points (m)	RMSE of control points (m)
Linear poly.	107.447	76.651
Bilinear ploy.	122.229	40.377
Quadratic (type 1)	97.196	34.971
Quadratic (type 2)	108.518	29.344

Table 6- 2D projective transformation result

Method	RMSE of check points (m)	RMSE of control points (m)
2D projective trans.	348.9126	412.698

Table 7- RMSE of check points obtained by DLT (method 1)

Method	X & Y RMSE of check points (m)	Z RMSE of check points (m)
DLT	124.513	413.665

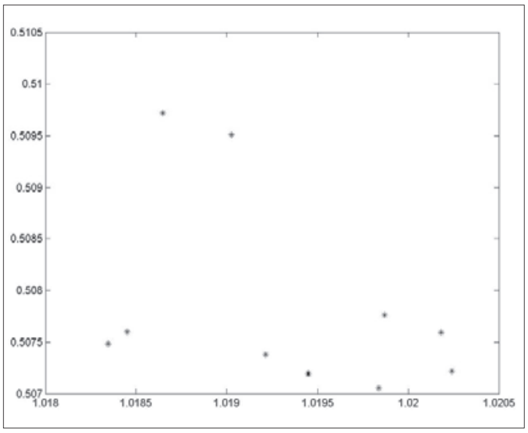

Fig. 5- Control and check points in blue and red, respectively.

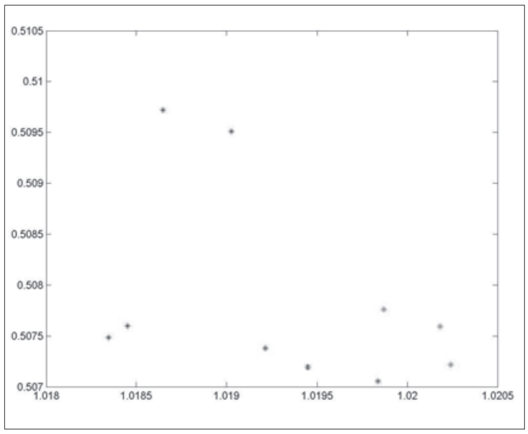

Fig. 6- Distributions of check and control points: green points are control ones located in flat area, blue points are represented the check points in mountainous area while the red ones illustrate the check points located in flat areas

Table 1- Information of SAR images used here

Information	Des. Image 1	Des. Image 2	Asc. Image
Product type	SLC	SLC	SLC
Sensor mode	Image	Image	Image
Source	ASAR	ASAR	ASAR
Acquisition date	2003/06/11	2003/12/23	2004/01/25
Product ID	ASA_IMS_1P	ASA_IMS_1P	ASA_IMS_1P
Orbit number	6687	9192	9958
Satellite ID	N1	N1	N1
Range Sample spacing in meters	7.80397463	7.80397463	7.80397463
Azimuth sample spacing in meters	4.050520072	4.050520072	4.050520072
Azimuth sample spacing in time	0.000605 (s)	0.000605 (s)	0.000605 (s)
Incidence angle in Near range	18.579622	18.572363	18.570648
Incidence angle in Far range	26.147577	26.142576	26.145206
Number of range lines	26888	26897	23588
Number of samples per range line	5167	5167	5170

Table 2- Results of different polynomials.

Polynomial type	RMSE of check points (m)	RMSE of control points (m)
Linear poly.	82.249	82.769
Bilinear ploy.	80.203	78.659
Quadratic (type 1)	59.357	57.808
Quadratic (type 2)	66.342	35.545
Quadratic (type 3)	57.370	56.307
Quadratic (type 4)	58.501	55.790

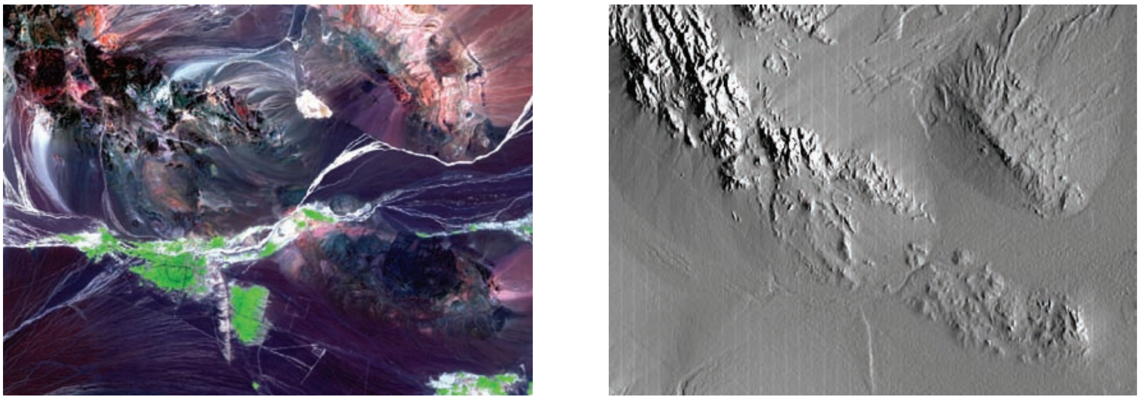

(a) (b)

Fig. 1- (a) ETM+ image and (b) shaded relief of the study area.

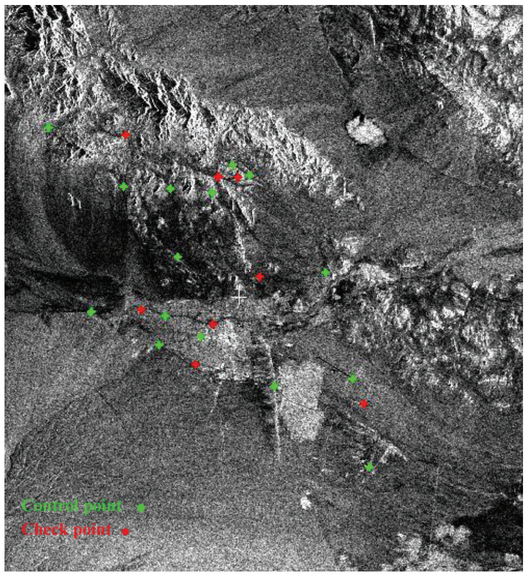

Fig. 2- Distribution of check and control points of 6687 SAR image in red and green, respectively.

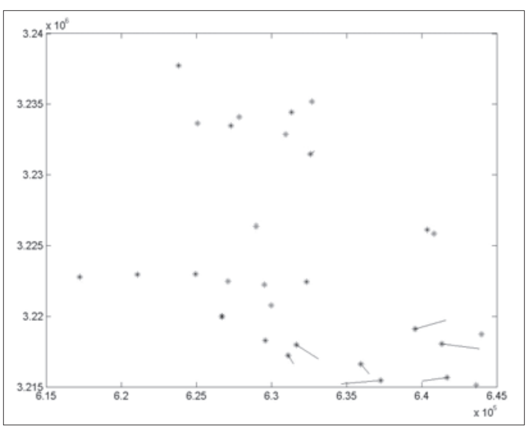

Fig. 3- Control and check points of images 6687 and 9192 in blue, green and red, respectively.

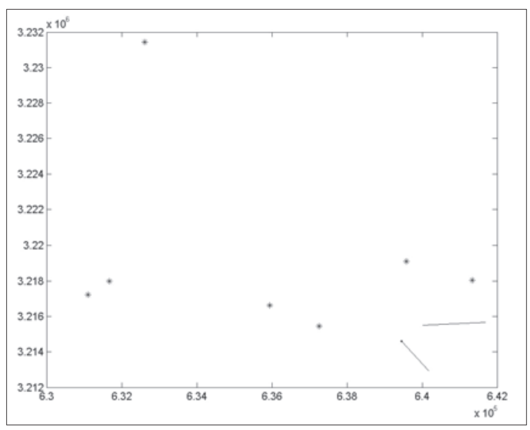

Fig. 4- Common control and check points of images 6687 and 9192 in blue and red, respectively.

$$(X - X_S)^2 + (Y - Y_S)^2 + (Y - Y_S)^2 = R^2 \tag{10}$$
$$(\dot{X} - \dot{X}_S)(X - X_S) + (\dot{Y} - \dot{Y}_S)(Y - Y_S) + (\dot{Z} - \dot{Z}_S)(Z - Z_S) = \frac{\lambda R f_D}{2}$$

where *(X, Y, Z)* is the unknown geographic position of the target point to be solved, *(X, Y, Z)* is the sensor position at the time of point acquisiti on, $(\dot{X}_s, \dot{Y}_s, \dot{Z}_s)$ is the velocity vector of the target point and $(\dot{X}_s, \dot{Y}_s, \dot{Z}_s)$ is the sensor velocity vector which can be determined by the attitude angles and moving speed of the sensor along the orbit. There are three unknown parameters *(X, Y, Z)* and two equations that are not sufficient to estimate the unknown parameters. Therefore a stereo pair of image should be used. However, in the ephemeris data available in this study, there was no information about the Doppler centroid. Hence, we were not able to establish the Doppler equation. In order to compute the unknown coordinates, instead of two images, three SAR images had to be used: two descending images and one ascending one.
In order to estimate the unknown SAR model parameters, totally 10 check and control points were captured in three images. 4 points were used as control points while 6 points were exploited as check points as shown in Figure 5.

It was found that to mix the points of different areas (flat and mountainous) results in inaccurate processing parameters. Therefore, the control points were selected in the flat area. Among the check points two are located in the flat area in the vicinity of the control points while the others are placed in the mountainous area.
The differences between the computed control and check points coordinates and their real values are given in Table 11.

In Figure 6, the control points are in green, check points in blue and those check points which are located in the flat area are depicted in red.

Considering the poor distribution of the GCPs, it is obvious that the model is not fitted appropriately to the mountainous area. Due to the lack of GCPs in the study area, it was not possible to fit a better model to the mountainous area.

5. Conclusions and Discussion

Applying the 2D math models, it was possible to correct SAR images without considering the imaging geometry. The results showed that the main part of the error existing in SAR images can be modeled through 2D polynomials. Since the SAR images used in this study are in slant range geometry, it was expected that considering the imaging geometry might lead us to the better results. In 3D geometric correction, the proposed SAR rigorous model exploited the available topographic data to calibrate the satellite ephemeris data. Using the refined SAR processing parameters, we were able to geocode the SAR imagery with an assumption that the used GCPs are error-free. The calibration was done by an iterative LS method applying the ephemeris data as initial values. As it was found, this method is very sensitive to the GCPs type. Since the points located in the flat areas were used for parameters refinement, the model was fitted to the flat area. However, in comparison with other methods, the results achieved by the rigorous SAR model were not accurate enough. The reasons would be:

1. The first and foremost reason is that the base to height ratio of the employed images was so small that the satellite configuration is poor. In order to obtain the required accuracy in DEM extraction, the baseline must be larger than 250 m. The more the baseline is, the more the accuracy of the extracted DEM is. However, in this study the baseline is less than 50 m. Because the available data was provided for the interferometry purpose.
2. Due to the lack of distinguishable features in the images and low radiometric quality of them, it was not possible to capture adequate control points.
3. Collecting of control points was a difficult task regarding inherent SAR error such as foreshortening and layover.
4. The available control points are not distributed uniformly in the study area.
5. The proposed rigorous SAR model is sensitive to the area type. If a model is fitted to the flat area, it can not be suitable for hilly or mountainous areas.
6. The last but not least is that the ephemeris data did not include any information about Doppler centroid. Therefore, we had to use one extra image (an ascending one) to make sufficient equations. To combine three images in order to extract the ground coordinates caused the image errors added together and made the results inaccurate.

As a final conclusion, in order to obtain more accurate results in rigorous SAR model, the images should be appropriate regarding the geometry and accessible ephemeris data. In case of lacking such proper information, using 2D polynomials would be recommended.

algorithms the homologous points are extracted (matching) and the operator plays the role of supervisor. In this study, the first approach was exploited. The entire Radargrammetry procedure consists of two main steps:

1- The accurate geometric correspondence between image and object space must be established refining SAR images parameters.
2- An inverse trisection problem must be solved to obtain the coordinates of each terrain points. The image coordinates of those points are found through a correlation process.

In order to establish the image to object correspondence, a rigorous SAR Image Formation Model (SIFM) must be defined. In this approach the model parameters whose accuracies are inadequate have to be refined based on calibration using control points.

4.2.2.1. SAR Image Formation Model (SIFM)

The model used here is based on two basic SAR mapping equations called range and Doppler equations as follows (Liu et. al., 2004):

$$R(t) = \sqrt{(\vec{S}(t) - \vec{P}(t)).(\vec{S}(t) - \vec{P}(t))} = \left|\vec{S} - \vec{P}\right| = SP$$
$$f_D = -\frac{2.\vec{SP}.\vec{V}_s}{\lambda.SP} \quad (5)$$

where $\vec{P}(t) = (X, Y, Z)$ and $\vec{S}(t) = (X_s, Y_s, Z_s)$ are the locations of the target point on the ground and the satellite, respectively. It should be noticed that these coordinates are stated in the earth-fixed coordinates system (CT). $\vec{V}_s(t) = (\dot{X}_s, \dot{Y}_s, \dot{Z}_s)$ is the satellite velocity vector, $R(t)$ is the slant range distance, f_D is the Doppler centroid frequency and λ is the radar wavelength. The SIFM includes different groups of parameters: orbital parameters, sensor parameters and SAR processing parameters.
Using at least three sets of satellite position vectors available in the satellite ephemeris data, the sensor position can be modeled by:

$$X_s = a_0 + a_1 t + a_2 t^2 + a_3 t^3$$
$$Y_s = b_0 + b_1 t + b_2 t^2 + b_3 t^3 \quad (6)$$
$$Z_s = c_0 + c_1 t + c_2 t^2 + c_3 t^3$$

where a_i, b_i, c_i $(i = 0, 1, 2, 3)$ are fitted coefficients.
The Doppler centroid varies along azimuth and range direction and can be approximated applying the satellite ephemeris data as follows:

$$f_D = d_0 + d_1 R + d_2 R^2 + d_3 t + d_4 t^2 \quad (7)$$

where d_i $(i = 0, 1, 2, 3)$ are fitted coefficients, R is the slant range and t is the time. For a given target the acquisition time t is related to the azimuth coordinate (lin) of the SAR image by:

$$t = t_0 + \Delta t.(lin - 1) \quad (8)$$

where Δt is the azimuth sample spacing in time which is related to the pixel spacing in azimuth direction and t_0 is the time acquisition of the first image line.
The slant range is related to the slant range coordinate (col) as follows:

$$R_s = R_{s0} + \Delta R.(col - 1) \quad (9)$$

where R_{s0} is the near slant range and ΔR is the pixel size in range. Some of the model parameters are known with inadequate accuracy. In order to obtain an accurate geolocation, these parameters must be refined by a Least Square calibration using GCPs. In this method we have to use a stereo pair of SAR images. The unknown parameters are: the near slant range R_{s0}, the acquisition time of the first image line t_0, the pixel size in range and azimuth direction ΔR and Δt ,respectively and the coefficients of the orbit polynomials. These parameters are considered constant in a SAR image scene. In order to obtain geometric consistency, the joint calibration was used to estimate the unknown parameters of two images simultaneously (block adjustment). The adjustment is carried out with a LS iterative procedure and the unknown parameters are estimated in a very good convergence. The total gradient in the convergence problem reached to 0.0000001 after 130 iterations.

4.2.2.2. Derivation of 3D coordinates of homologous points by space resection

With the image coordinates (lin_i, col_i), of the target point, two SAR equations can be formed (Crosetto, et. al.). By rewriting the range and Doppler equations we obtain:

4.2. 3D Geometric correction

There are different approaches in order to do 3D geometric correction of the image. These models is mostly used in order to orthorectify the satellite images (relief displacement reduction) or to generate the DEM. For DEM generation after 3D math model definition, a stereo pair of images is needed. While working with SAR data, two images acquired from different positions in the space are exploited. The distance between two acquisition stations is called baseline. The larger the baseline is, the more accurate the extracted DEM is. In the following sections several techniques are introduced and tested on SAR data.

4.2.1. Direct Linear Transformation (DLT)

The first step in using this method is to define the appropriate model for two descending images (6687 and 9192) and the second one is to exploit two images in order to compute the height corresponding to each point. DLT transformation is a special case of 3D projective transformation defined as follows:

$$x = \frac{L_1 X + L_2 Y + L_3 z + L_4}{L_9 X + L_{10} Y + L_{11} z + 1}$$

$$y = \frac{L_5 X + L_6 Y + L_7 z + L_8}{L_9 X + L_{10} Y + L_{11} z + 1} \quad (4)$$

This method has been used in to different ways:

1. Coefficients estimation of each image separately: employing 16 and 13 GCPs for images 6687 and 9192, respectively, DLT coefficients for each image were estimated separately. In order to test the results, 8 common check points of both images (homologous points) were selected and the ground coordinates including X, Y and Z were calculated. The results are given in Table 7.

The differences between the computed and original coordinates of check points are given in Table 8.

AS it can be observed, the accuracy of X, Y and specially Z is very low. The reasons may be:

-The baseline is very small due to the SAR images used. Normally it must be more than 250 m for obtaining required precision in height estimation. However the baseline is less than a couple of 10 meters. Therefore, the satellite configuration does not have the required consistency. This fact affects the accuracy of the results.

-The quality of GCPs is relatively low.

-The last but not least is that the control and check points do not have the satisfying distributions due to the lack of homologous points.

In Figure 3, the control points of images 6687 and 9192 are shown in blue and green while the check points are illustrated in red.

For more geometric consistency, the images should be modeled together using the same control points. Therefore, it is preferred to apply the second method.

2. Using homologous points of these two images and coefficients estimation of both images together: in this method two images are modeled simultaneously using 7 GCPs and 2 check points. The results are shown in table 9.

The differences between the computed and original coordinates of check points are depicted in table 10.

It should be noted that there is one check point common in evaluating both methods which is highlighted in Tables 8 and 10. Although the number of used GCPs in the second approach is much less than the first one, the results are more reliable. Figure 4 illustrates the distribution of GCPs and check points. The better results in 3D geometric correction can be obtained while considering the imaging geometry at the time of imaging. Since the SAR imaging is different from other types of sensors, a specific model is needed for SAR geometric correction. In the following section a rigorous geometric SAR model will be presented.

4.2.2. Radargrammetry – a Rigorous Geometric SAR Model

By the advent of SAR data, new algorithms have been developed to generate DEM. Starting from SAR images, DEM can be produced using either the amplitude (radargrammetry or shape from shading techniques) or phase (interferometry). Radargrammetry is the technology of extracting geometric object information from radar images (Leberl, 1990). Radargrammetry uses amplitude SAR images applying the same approach that photogrammetry uses with optical images. This technique is employed with stereoscopic pairs acquired from the same side but with different incidence angles. Radargrammetry can be implemented using an interactive approach or an automatic one. In the former method, the operator must capture the data manually while in the latter based on image correlation points of the first descending image (6687) used in 2D geometric correction.

4.1.1. Interpolative Models

This method corrects the images geometrically without considering the imaging geometry at the time of imaging. A math model which is mostly a polynomial is applied to relate the image and ground space.

Using the first data set of 6687 descending SAR image, the best polynomial fitted to the area was selected according to the check points RMSE (Root Mean Square Error) using different interpolative methods. It should be noticed that before geometric correction the image was downsampled to the resolution of 20 meters. Among 24 points selected from the topographic map, 15 points were used as control points and the rest of them were considered as check points. The 2D math models tested on the image are as follows:

1. Global polynomial: In this method one general 2D polynomial is fitted to the whole image. As mentioned before the best polynomial is selected based on the RMSE of the check points. Several polynomials were tested including Linear, Bilinear and different forms of quadratic one. The results are depicted in Table 2.

As it can be seen, the best polynomial fitted to the image is quadratic type 3 defined as follows:

Quadratic type 3:

$$
\begin{aligned}
X &= a_0 + a_1 x + a_2 y + a_3 xy + a_4 x^2 + a_5 x^2 y \\
Y &= b_0 + b_1 x + b2 y + b_3 xy + b_4 x^2
\end{aligned} \tag{1}
$$

2. Point wise: In this model after selection of the best global polynomial, the computed coordinates of each unknown point will be corrected based on a couple of effective control points selected based on different strategies. The simplest strategy to select the effective control points is based on their nearness to the unknown point. This method was tested using different number of effective control points. In order to refine the calculated coordinates, based on the effective control points, two different methods called moving average and weighted distance were applied. As a result the residual vectors should be reduced in each unknown point. Table 3 shows the results of point wise method applying different number of effective points which are the nearest ones.

As it is shown in Table 3, the point wise results are not satisfying as it was expected before. The reason is that the effective control points selection strategy which was based on the distance is not proper enough in this image because the image is a mixture of various types of area. It is mostly preferred to take a supervised method to select the effective control points.

3. Piece wise: Since the image is a mixture of several regions with different topographic characteristics, a unique polynomial can not be fitted very well to the whole image. Therefore, the most proper thing to do is to split the image into different regions and fit a specific polynomial to each part of the image. The image 6687 is a combination of hilly and flat areas. Hence, different polynomials were tested to each area separately. The results are given in Tables 4 and 5. According to these tables, the best polynomials fitted to the flat and mountainous areas are quadratic type 3 and 1, respectively as shown in Eqs. (1) and (2).

Quadratic type 1:

$$
\begin{aligned}
X &= a_0 + a_1 x + a_2 y + a_3 x^2 \\
Y &= b_0 + b_1 x + b2 y + b_3 x^2
\end{aligned} \tag{2}
$$

4. 2D projective transformation: The mathematical model used here is as follows:

$$
\begin{aligned}
x &= \frac{L_1 X + L_2 Y + L_3}{L_7 X + L_8 Y + 1} \\
y &= \frac{L_4 X + L_5 Y + L_6}{L_7 X + L_8 Y + 1}
\end{aligned} \tag{3}
$$

This method assumes that the height difference in the area is zero. However, our study area does not have such a characteristic. Therefore, it is expected not to get satisfying results using this algorithm.

The results shown in Table 6 prove our claim.

4.1.2. Parametric models

This model considers the imaging geometry. Each error source is recognized and modeled in this method. Then the imaging geometry is corrected regarding the modeled errors. Since, the recognition and modeling of all errors is impossible, this method is rarely used. In our study this method is ignored due to the mentioned reason.

1. Introduction

A SAR (Synthetic Aperture Radar) is a distance-measuring device. The RADAR system measures the time delay between transmission and reception of a pulse in order to determine the target's location with respect to another one in the range direction. This kind of data recording causes spatial distortions in SAR data. When a satellite SAR is imaging a steep relief feature such as a mountain, the RADAR pulse could reach the top of the mountain first and the bottom of the mountain last. Therefore, from the SAR's perspective, the top of the mountain is closer than the base of the mountain. As a result the mountain appears to be leaning toward the sensor, causing the displacement of mountain tops and other topographic features from their orthographic positions. These distortions make SAR data completely different from other remotely sensed data type, and consequently the SAR sensor model differs form optical sensor models. In this paper, in order to model the spatial distortions in the SAR images, different approaches were applied. In the next section the study area and the data used are introduced. Section 2 presents the preprocessing steps which are essential to preparing data. Section 3 is devoted to geometric correction including 2D and 3D math models. Some concluding remarks are given in the last section.

2. Study area and available SAR data

In this study, different math models were tested with ENVISAT ASAR (Advanced Synthetic Aperture Radar) data of Bam area. There are different ASAR products available for different applications. The product used here is Image Mode Single-Look Complex (ASA_IMS_1P). Image Mode Single-Look Complex is phase-preserved image generated using up-to-date auxiliary parameters. Auxiliary data is essential to processing which is used to produce a product. These data may include calibration data measured on-board but is not part of the main measurement data of the instrument. It may also include external calibration files from sources other than the satellite, processor configuration files, and any other files needed by instrument processor. Generally, these types of product are called SLC. These data cannot be used directly unless a couple of pre-processing procedures have been done on them. In order to prepare SAR data, Basic ENVISAT SAR Toolbox (BEST) was applied. This software is a widely used package for ENVISAT data pre-processing and preparing them for further processing.

There were 3 SLC images available for BAM area. Two of them were acquired in descending mode, while the third one's acquisition mode is ascending. Two descending images nearly cover the same area since the baseline is a couple of ten meters which is small. However, since the acquisition geometry of the ascending mode is different, the overlapped area between them are very small. Bam city is located in a relatively flat area. In north of Bam there is a mountainous area which is subject to foreshortening, layover and shadow. Figure 1 illustrates the ETM^+ image and shaded relief of the study area extracted from SRTM DEM.

3. Pre-processing SAR data

As mentioned before BEST software was applied for preparing SAR data. In this step after full resolution SAR image extraction using header information, the complex image is converted in to amplitude.

Since SAR is a coherent imaging system, the image is subject to speckle noise, which reduces the image quality. In order to reduce the speckle noise an adaptive filter called Lee with the window size of 3 was used.

Table 1 shows the SAR images information used in this study.

After pre-processing step, different math models including 2D and 3D models are applied on the images and the results are compared together.

4. Geometric correction

The first and foremost step in geometric correction is Ground Control Points (GCPs) collection. The most suitable GCPs sources available here is digital topographic map of the area with the scale of 1:25,000. The projection system is UTM and the area is located in zone 40. The reference ellipsoid is WGS84. For 3D math models, elevation information was extracted using SRTM DEM with the resolution of 80 m. Although the used DEM is very course compared to SAR data, the height accuracy is quite acceptable. In this section numerous mathematical models will be tested on SAR images.

4.1. 2D geometric correction

The images are corrected with respect to the x and y coordinates using 2D geometric correction models. There are two general types of 2D math models which are explained in the following sections.

Figure 2 shows the distribution of the control and check

بررسی مدلهای ریاضی دو بعدی و سه بعدی برای تصحیح هندسی تصاویرراداری SAR (مطالعه موردی در منطقه بم)

نوشته: مریم دهقانی*، محمد جواد ولدان زوج* علی منصوریان*

*دانشکده مهندسی ژئودزی و ژئوماتیک، دانشگاه صنعتی خواجه نصیرالدین طوسی، تهران، ایران

Study of 2D and 3D Geometric Models Applied on SAR Images (A case study in BAM area)

By: M. Dehghani*, M. J. Valadan Zouj* & A. Mansourian*

*Faculty of Geodesy & Geomatics Engineering, K. N. Toosi University of Technology (KNTU), Tehran, Iran.

تاریخ دریافت: ۱۳۸۵/۰۹/۱۸ تاریخ پذیرش: ۱۳۸۵/۱۱/۱۸

چکیده

در این مقاله، انواع مدلهای ریاضی دوبعدی و سه بعدی به منظور تصحیح هندسی تصاویر SAR در هندسه Slant range استفاده شده است. تعدادی از این مدلها، هندسه تصویر را در لحظه تصویربرداری در نظر می‌گیرند، در حالی که دیگر مدلها، فضای تصویررا به کمک یک چند جمله‌ای با فضای زمین مرتبط می‌سازند. تصاویر مورد آزمایش، سه تصویر ENVISAT از منطقه بم است. برای تصحیح نقاط کنترل دو بعدی از نقشه توپوگرافی با مقیاس ۱:۲۵۰۰۰ و ارتفاع آنها از SRTM استخراج شدند. مدلهای استفاده شده در روش دو بعدی انواع چندجمله‌ایها، piece wise ،point wise و projective بوده در حالی که برای تصحیح هندسی سه بعدی مدل پیچیده SAR به کارگرفته و نتایج آن با روش DLT مقایسه شد. از آنجا که این تصاویر به منظور مطالعات تداخل سنجی تهیه شده‌اند، خط مبنای آنها کوچک بوده و در نتیجه دقت استخراج مختصات سه بعدی به کمک زوج تصویر آنها پایین است. در حالی که نتایج تصحیح هندسی دو بعدی از دقت نسبتاً خوبی برخورداراست.

کلید واژه‌ها: رادار، تصاویر SAR، تصحیح هندسی، نقطه کنترل، رادارگرامتری

Abstract

study several 2D and 3D math models have been tested in order to correct slant range SAR data geometrically. Some of these models consider the imaging geometry at the time of imaging while the others relate the ground space to the image one by mathematical polynomials. The images used here are 3 ENVISAT ones of Bam area. In order to extract the 3D GCPs, a topographic map with a scale of 1:25000 and SRTM DEM were used. The 2D math models used in this study include Global polynomial, Point wise, Piece wise and Projective while the 3D models are DLT and Rigorous SAR model. Since the images used in this study were originally ordered for interferometry studies, their baseline is so small that the precision of 3D coordinates extraction is not satisfactory enough. However, the results of 2D models are much better.

Key words: RADAR, SAR images, Geometric correction, Control point, Radargrammetry

راهنمای نگارش مقاله

۱- مقاله ارائه شده در ارتباط با زمین‌شناسی و علوم زمین باشد.

۲- مقاله دارای نوآوری بوده و نویسنده متعهد شود برای نخستین بار،در فصلنامه علوم زمین ارائه شده است. صحت و سقم این مطلب با مسئولیت نویسنده است.

۳- مقاله در نرم افزار Word نسخه 2003 یا XP تایپ شود.

۴- از آنجا که قالب بندی فصلنـــــــامه، پس از داوری، ویرایش و انجام اصلاحات نهایی در مقالات اعمال می‌شود، در نسخهٔ اولیه ارسالی، فاصله‌ها از هر چهار طرف ۳ سانتی متر و فاصله سطرها ۱/۵ برابر در نظر گرفته شود. تمامی متن مقاله نیز در یک ستون تنظیم گردد.

۵- در تمام متن فارسی از قلم Zar و قلم انگلیسی Times New Roman استفاده شود. اندازهٔ فونت فارسی برای عنـــوان مقاله زر ۱۶ و برای تیترهـای اصلـی و فـــرعی زر ۱۴ و برای متن قلم زر ۱۳ در نظر گرفته شود. اندازه فونت انگلیسی، دو شماره کوچک‌تر از فونت فارسی باشد.

۶- تیترها(اصلی و فرعی) شماره گذاری شوند. شماره اصلی در سمت راست و شماره فرعی در سمت چپ قرار می‌گیرد. برای مثال قسمت سوم از بخش پنجم مقاله به صورت ۵-۳ نوشته می شود.

۷- در صورت نیاز به ذکر واژه‌های انگلیسی همزمان با مترادف فارسی و برای تنهـا یـک بـار در متن در داخـل پرانتـز آورده شـود. (از آوردن مترادفهـا و توضـیحات بـه صـورت زیرنویس صفحات خود داری شود).

۸- در تمام متن "ها" جمع پیوسته، "تر" و "ترین" جدا نوشته شود.

۹- در هنگام ارجاع به مراجع در داخل متن، برای مراجعی که به زبان انگلیسی نوشته شده‌اند ، نام نویسنده و سال انتشار با حـروف انگلیسـی و مراجـــع فارسـی بـا حـروف فارسـی نوشته شود (از ذکر شماره مرجع مورد نظر به جای نام نویسنده و سال انتشار خودداری شود). کلیه مراجع فارسی و انگلیسی در بخش کتابنگاری، بر اسـاس حـروف الفبـا مرتـب شوند.

۱۰- الگوی مرجع نویسی در بخش کتابنگاری با توجه به نمونه‌های زیر و رعایت حروف بزرگ و ایتالیک نوشته شود:

۸ -۱- مقالات:

سهیلی، م.، ۱۳۶۱- شرح نقشه زمین شناسی نیمه جنوبی چهارگوش کوه کورخود، سازمان زمین شناسی کشور، ۱۱۰ صفحه

Batchelor, R.A. & Bowden P. , 1985- Petrogentic interpretation of granitoid rock series using multicationic parameters, chemical geology, 48: 43-55.

۸- ۲- کتاب:

Wetzel R.G., 1983- Limnology, 2nd edition. Saunders publishing company, 582 p.

۸-۳- مقاله‌های مندرج در مجموعه مقالات یا کتابهای چند نویسنده :

Smith A.C.S. & Mudder T.I., 1999- The environmental geochemistry of eyanide. in : Plumlee G.S., & Logsdon M.J. (eds.) The Environmental Geochemistry of Mineral Deposits. Society of Economic Geologists. PP2q-z48

۱۱- کلمه‌ها و متون داخل جدولها و شکلها تا حد امکان فارسی شود.

۱۲- در صورت نیاز، جدولها راست به چپ باشند.

۱۳- مقاله ارسالی به فصلنامه بایستی نسخه اصلی (پرینت اصلی با شکلهای رنگی) همراه با نشانی کامل نویسنده (مسئول مکاتبات)، شماره تلفن (ترجیحا تلفن همـراه) و نـشانی پـست الکترونیکی باشد.

۱۴- در مقالات انگلیسی، ذکر عنوان مقاله، نام نویسندگان، محل کار نویسندگان، چکیده و کلید واژه‌ها به فارسی الزامی است.

۱۵- مقاله، در چهار نسخه (یک نسخه اصلی همراه با ذکر مشخصات کامل نویسندگان و محل کار آنها و سه نسخه بدون نام و محل کار نویسندگان) ارسال گـردد. در صـورتی کـه مقاله نیاز به اصلاحیه داشته باشد، مقاله اصلاح شده در دو نسخه (یک نسخه با ذکر مشخصات کامل نویسنده و یک نسخه بـدون مشخـصات نویـسنده) بـه دفتـر فـصلنامه ارسـال گردد. در صورت وجود هرگونه نقص در مدارک، مقاله عودت داده می‌شود.

۱۶- در مقالات ارسالی ترتیب زیر رعایت شود: الف) عنوان فارسی ب) عنوان انگلیسی پ) اسامی نویسندگان به فارسـی و انگلیـسی ت) چکیـده فارسی ث) کلید واژه‌ها به فارسی ج) چکیده انگلیسی (Abstract) چ)کلید واژه‌ها به انگلیسی (Kay words) ح) محل کار نویسندگان به فارسی و انگلیسی خ) مقدمه د) متن مقاله ذ) بحث و نتیجه گیری ر) تشکر و قدردانی ز) فهرست مراجع(کتابنگاری)

۱۷- تعداد صفحات مقاله (چکیده، متن مقاله، مراجع، شکلها و نمودارها) در مجموع نباید بیش از ۱۵ صفحه باشد. صفحات مقاله نیز بایستی شماره گذاری شوند. از فرستادن جدولها، زیرنویس شکلها و زیر نویس جدولها به صورت JPG خودداری گردد. موارد ذکر شده بایستی در Word تنظیم شده باشند.

۱۸- در متن مقاله، اختصاص یک بخش به روش مطالعه الزامی است .

۱۹- ارسال CD حاوی فایل کامل مقاله (به صورتی که ذکرشد)، لازم بوده و بایستی پس از اخذ نامهٔ پذیرش، و اعمال کلیهٔاصلاحات پیشنهادی داوران، صورت گیرد.

۲۰- به منظور غنی ساختن بانک اطلاعاتی داوران مربوط به هر گرایش، به همراه مقالهٔ ارسالی، اسامی حداقل پنج نفر از کسانی که در همان زمینهٔ تخصصی فعالیت داشته‌اند، به همراه نشانی پست الکترونیک، نشانی دقیق پستی، محل کار و تلفن (ترجیحاً تلفن همراه) قید شود. یادآور می‌شود این اسامی تنها جهت تکمیل بانک اطلاعاتی فصلنامه بـوده و لزومـی برای داوری مقاله توسط داوران معرفی شده وجود ندارد.